

High Efficiency Isolated Resonant Converter for Photovoltaic Applications

Nandisha L¹ and H.V. Govinda Raju²

¹4th semester, M.Tech (Power Electronics) Dr. Ambedkar Institute of Technology, Bengaluru, Karnataka, India

¹Dr. Ambedkar Institute of Technology, Bengaluru, Karnataka, India

E-mail: ¹nandishreddyl@gmail.com, ²govind.raju37@yahoo.com

Abstract---This paper presents Modular photovoltaic power conditioning systems (PCSs) require a high-efficiency dc-dc converter stage capable of regulation over a wide input voltage range for maximum power point tracking. In order to mitigate ground leakage currents and to be able to use a high-efficiency, nonisolated grid-tied inverter, it is also desirable for this microconverter to provide galvanic isolation between the PV module and the inverter. This paper presents a novel, isolated topology that is able to meet the high efficiency over a wide input voltage range requirement. This topology yields high efficiency through low circulating currents, zero-voltage switching (ZVS) and low-current switching of the primary side devices, ZCS of the output diodes, and direct power transfer to the load for the majority of switching cycle. This topology is also able to provide voltage regulation through basic fixed-frequency pulsewidth modulated (PWM) control. These features are able to be achieved with the simple addition of a secondary-side bidirectional ac switch to the isolated series resonant converter. Detailed analysis of the operation of this converter is discussed along with a detailed design procedure. Experimental results of a 300-W prototype are given. The prototype reached a peak power stage efficiency of 98.3% and a California Energy Commission (CEC) weighted power stage efficiency of 98.0% at the nominal input voltage.

1. INTRODUCTION

Photovoltaic energy has been the fastest growing renewable energy source in recent years and is expected to continue this trend throughout the near future. In order for the solar energy market to continue this growth and to become more competitive with traditional energy sources and other forms of renewables, both PV panels and PV power conditioning systems (PCSs) need to be designed to perform more efficiently while becoming lower in cost. The subject matter of this paper focuses on improvement of the performance of the electronics involved in the PCS. There are three main types of PV PCS configurations: centralized, string, and modular. The first two configurations are comprised of several series- or parallel-connected PV modules that are fed into a large centralized inverter or several smaller string inverters. These configurations suffer from the inability to have each individual PV module operating at its own maximum power point, but are relatively cheap to implement

and therefore are more common in today's PV installations. PV modules exhibit nonlinear power output characteristics that may differ for each module depending on the PV cell material and environmental conditions such as temperature, solar irradiance, dirt and debris collected on the panels, etc. Because the optimal operating point may differ for each module at any given time, it is desirable for each panel to have its own power optimizing electronics implementing a maximum power point tracking (MPPT) algorithm. The third type of PV PCS configuration is comprised of several PV modules, each with its own power converter, or module integrated converter (MIC), which tracks the MPP of each module individually and either outputs ac directly to the grid (microinverter) or outputs dc (microconverter), which can be connected in series or parallel with other microconverters to feed a centralized or string inverter. These modular configurations are very attractive because of more efficient energy harvesting and simple scalability.

2. BASIC BLOCK DIAGRAM

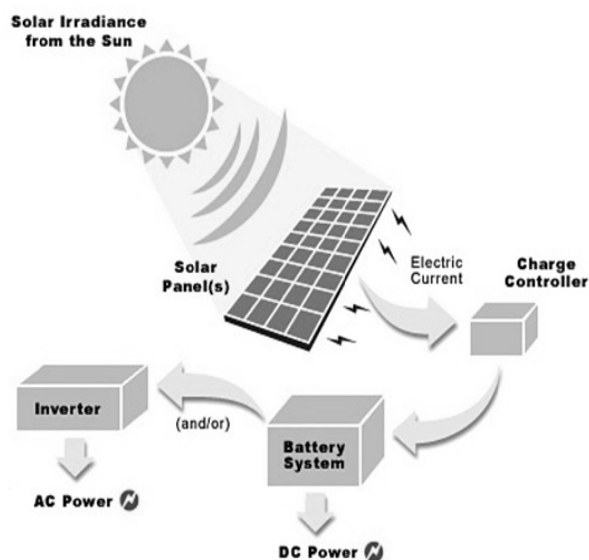


Fig. 1: Electricity generation from PV cells

Photovoltaics are best known as a method for generating electric power by using solar cells to convert energy from the sun into a flow of electrons. The photovoltaic effect refers to photons of light exciting electrons into a higher state of energy, allowing them to act as charge carriers for an electric current. The photovoltaic effect was first observed by Alexandre-Edmond Becquerel in 1839. The term photovoltaic denotes the unbiased operating mode of a photodiode in which current through the device is entirely due to the transduced light energy. Virtually all photovoltaic devices are some type of photodiode.

3. METHODOLOGIES

The proposed converter is shown in Fig. 2. The topology is very similar to an isolated resonant converter with a voltage doubler output similar to what is discussed in, except for the addition of a bidirectional ac switch, S_5 , across the secondary winding of the isolation transformer. In the figure, S_1 through S_4 on the primary side of the isolation transformer make up a full-bridge switch network that could also be implemented as a half-bridge or push-pull network in order to reduce switch count. This switch network operates at the series resonant frequency, f_r , which is determined by the resonant inductance, L_r , and resonant output capacitors, C_{r1} and C_{r2} , assuming L_m is much larger than L_{rand} and C_o is much larger than C_{r1} and C_{r2} . This allows the converter to act as a series resonant converter when S_5 is not used. L_{rcan} can either be the leakage inductance of the isolation transformer or the series combination of the leakage with an external resonant inductor. n and L_m are the turns ratio and magnetizing inductance of the transformer, respectively.

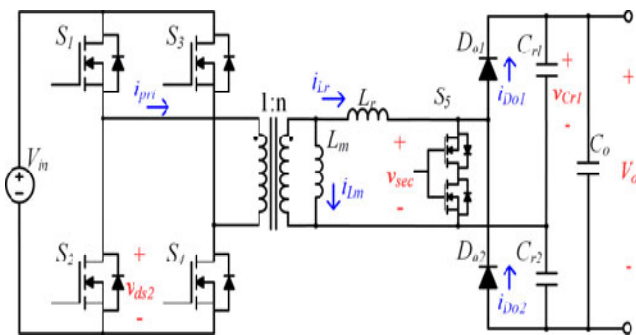


Fig. 2: Topology of proposed resonant converter.

S_5 is a bidirectional ac switch. For this application, it is implemented as two drain-connected MOSFETs. The duty cycle of S_5 , d_{ac} , is the control input variable so the switching frequency will be defined as the periodic frequency at which S_5 is switched, which is equal to twice the resonant frequency. When this switch is on, it shorts out the secondary transformer winding and the leakage inductance acts as a boost inductor. When the ac switch turns off, the leakage inductance then resonates with the resonant capacitors. This operation allows the initial conditions of the resonant trajectory to be set, allowing the power flow and conversion ratio to be controlled.

4. CIRCUIT OPERATION

The expected operation is as below:

MOSFETs S_1, S_2, S_3, S_4 are made to work in sequence and in pairs by providing Gating signals with appropriate duty cycle “D”. Since they are rated for higher voltage, MOSFETs can give higher drain voltage at the primary side. The drain current builds gradually and finally a sinusoidal waveform appears at the primary of the transformer.

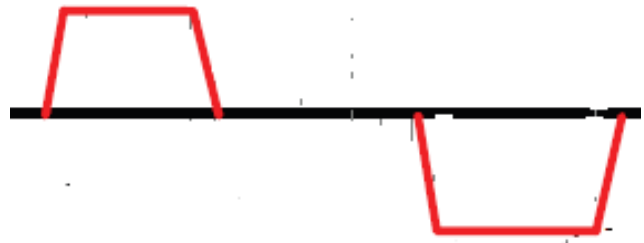


Fig. 3: Voltage at the primary of transformer

The voltage across secondary depends on the transformer turns ratio “n” and duty cycle “D”. This is an dc-ac conversion process. The ac-dc conversion process happens at the secondary of the transformer. The diodes at secondary as rectifiers and Capacitors helps in doubling the voltage and filtering also.

5. DESIGN PARAMETER

1. AC Switch Gating Scheme to Reduce Switching Losses

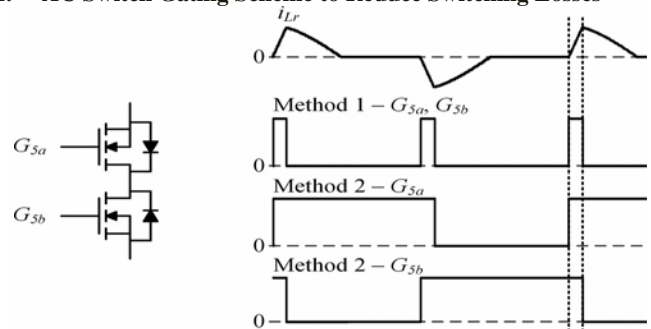


Fig. 4: Comparison of ac switch gating schemes.

It is possible to reduce the switching losses in the ac switch by controlling each of the gates separately when the device is comprised of two separate FETs or has two available gate pins. The device only needs to block voltage in one direction at a time, so it is possible to leave the other gate turned on when it does not need to block. Rather than turning both devices on for a short period of time as first introduced in Section II-B, it is possible to control the on time of the ac switch by controlling the overlap time of the two halves of the device. This is demonstrated in Fig. 4 where the gating scheme discussed in Part B is defined as Method 1 and the

reduced-switching-loss scheme is defined as Method 2. The power stage functionality of the converter is identical between the two methods, but the effective switching frequency of the ac switch is reduced by half.

2. Transformer Turns Ratio Selection

The most efficient operating point of the proposed converter will be when it is operating as a series resonant converter. This will happen when the duty cycle of the ac switch is zero, so the transformer turns ratio should be chosen so that the nominal input voltage will yield the proper output voltage. The formula for choosing the turn's ratio is shown in equation (1). If the converter's input voltage is above the nominal voltage, the ac switch duty cycle will be zero while the primary side devices are switched using pulse-width or phase-shift modulation to yield a conversion ratio less than that of the series resonant converter. If the converter's input voltage is below the nominal voltage, the switch can be utilized to yield a conversion ratio greater than the series resonant converter.

$$n = V_o/2V_{in-nom} - \quad (1)$$

3. Resonant Tank Design

The first step in designing the resonant network is to choose the resonant inductance, L_r . L_r should be as large as possible while not violating three upper limit constraints: the combined length of modes 1 and 2 must be less than or equal to the switching period, the voltage ripple across the resonant capacitors must not be too large, and practicality of physical transformer design unless there will be an external resonant inductor. This design step varies substantially from the design procedure of the LLC converter, where L_r is chosen based on a ratio between the leakage and magnetizing inductances that will yield the proper conversion ratio within the desired switching frequency range. For the proposed topology, L_r is independent of the desired conversion ratio because it acts as a PWM boost inductor operating at a fixed frequency.

Once L_r is chosen, C_r can be chosen accordingly based on the desired resonant frequency. Once C_r is chosen, a check needs to be performed to ensure that the resonant capacitor ripple will not be larger than the dc voltage across the capacitor, which is equal to half of the output voltage. Equation (2) shows what the minimum value that C_r can be as well as what the theoretical maximum value for L_r can be. Also, as it will be seen in the next subsection, the capacitor voltage ripple will affect the voltage rating of the ac switch, so even if C_r and L_r meet the criteria in (2), it may be desirable to select a larger C_r and smaller L_r in order to reduce the voltage stress across both S_5 and C_r

$$C_r > P_o T_s / V_o^2, L_r < V_o^2 / 2\omega_r^2 P_o T_s - \quad (2)$$

The final design constraint limiting the maximum value of L_r is the physical transformer design. The leakage inductance of the transformer can be increased by physically separating the primary and secondary windings with a split bobbin, but the achievable inductance may be smaller than what was desired

from the previous calculations. After the transformer is built this subsection may need to be revisited.

Table 1: Power stage parameters

Element	Value
F_s	130 kHz
S_1-S_4	Infineon IPB030N08N3
S_5	2x EPC EPC2010
d_{ac} range	0 - 0.28
D_{o1}, D_{o2}	Diodes Inc. PDU540-13
XFMR Core	Ferroxcube RM14/I-3C95
n	5.25
n_1	4 turns, 1.8 mΩ
n_2	21 turns, 38 mΩ
L_m	713.3 μH
L_r	33.5 μH
C_{r1}, C_{r2}	100 nF
C_o	1.2 μF
C_{in}	88 μF

6. EXPERIMENTAL RESULTS

A 300-W prototype was developed to experimentally verify the proposed converter and analysis. This prototype was designed to have an input voltage range of 15–55 V with a maximum power point operating range of 20–40 V and a nominal input of 30 V. The transformer turns ratio was selected so that for an input voltage of 30.5 V and less, the converter will be operating under the normal ac switch operation. For input voltages above 30.5 V, the ac switch is not used and the primary full-bridge switch network operates under phase-shift modulation. The proceeding experimental results discussion will be focused on the normal operating mode of the proposed converter, which is when the ac switch is used to achieve regulation. The output of the converter is chosen to be 320 V, which is sufficient for supplying a 120-Vac or 208-Vac inverter. Texas Instrument's TMS320F28027 Digital Signal Processor (DSP) was used for control implementation. A simple input voltage controller was implemented using a proportional integrator (PI) compensator. Parameters for the designed converter are given in Table I and photograph of the prototype is shown in Fig. 8. L_r is only the leakage inductance of the transformer so only a single magnetic device was necessary. Gallium nitride (GaN) MOSFETs were chosen for the ac switch implementation because, unlike the primary side MOSFETs, the ac switch does not achieve ZVS or ZCS. The outstanding switching characteristics of the GaNFET help to minimize these hard switching losses.

7. POSSIBLE OUTCOMES

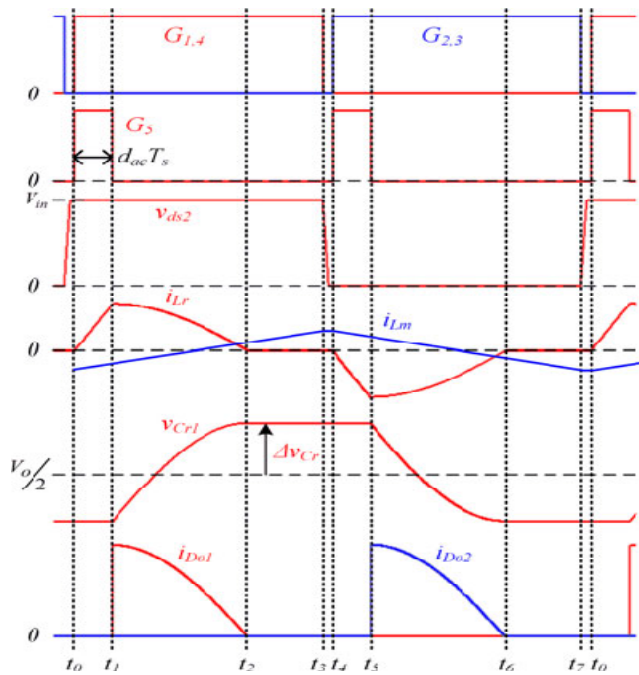


Fig. 5: Steady-state operating waveforms of proposed converter.

Simulation Results of the Converter

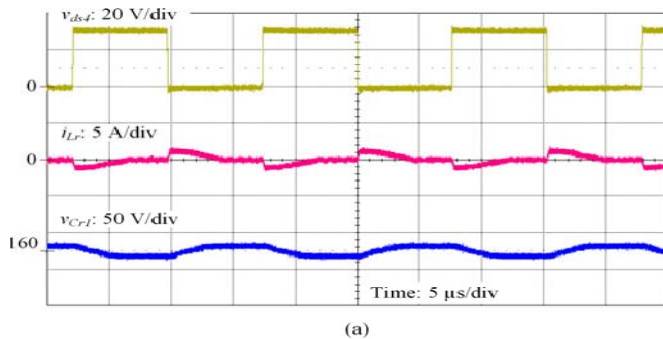


Fig. 6: (a) 30-V input and 60-W output,

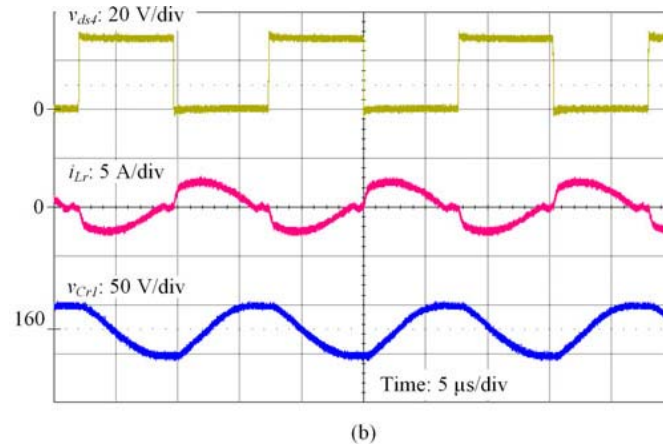


Fig. 6: (b) 30-V input and 225-W output,

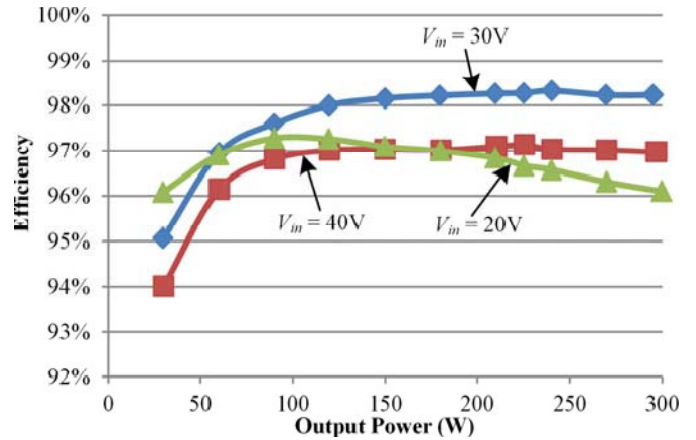


Fig. 7: Measured power stage efficiency of prototype for different input voltages

REFERENCES

- [1] F. Blaabjerg, Z. Chen, and S. B. Kjaer, "Power electronics as efficient interface in dispersed power generation systems," *IEEE Trans. Power Electron.*, vol. 19, no. 5, pp. 1184–1194, Sep. 2004.
- [2] Q. Li and P. Wolfs, "A review of the single phase photovoltaic module integrated converter topologies with three different DC link configurations," *IEEE Trans. Power Electron.*, vol. 23, no. 3, pp. 1320–1333, May 2008.
- [3] M. A. G. de Brito, L. Galotto, L. P. Sampaio, G. de Azevedo e Melo, and C. A. Canesin, "Evaluation of the main MPPT techniques for photovoltaic applications," *IEEE Trans. Ind. Electron.*, vol. 60, no. 3, pp. 1156–1167, Mar. 2013.
- [4] W. Yu, J.-S. Lai, H. Qian, and C. Hutchens, "High-efficiency MOSFET inverter with H6-type configuration for photovoltaic nonisolated AC-module applications," *IEEE Trans. Power Electron.*, vol. 26, no. 4, pp. 1253–1260, Apr. 2011.
- [5] R. Watson, F. C. Lee, and G. C. Hua, "Utilization of an active-clamp circuit to achieve soft switching in flyback converters," in *Proc. 25th Annu. IEEE Power Electron. Specialists Conf., (PESC '94) Record.*, 1994, vol. 2, pp. 909–916.
- [6] T.H. Hsia, H.-Y. Tsai, D. Chen, M. Lee, and C.-S. Huang, "Interleaved active-clamping converter with ZVS/ZCS features," *IEEE Trans. Power Electron.*, vol. 26, no. 1, pp. 29–37, Jan. 2011.
- [7] R. Beiranvand, B. Rashidian, M. R. Zolghadri, and S. M. H. Alavi, "Using LLC resonant converter for designing wide-range voltage source," *IEEE Trans. Ind. Electron.*, vol. 58, no. 5, pp. 1746–1756, May 2011.
- [8] H. Hu, X. Fang, F. Chen, Z. J. Shen, and I. Batarseh, "A modified high efficiency
- [9] LLC converter with two transformers for wide input-voltage range applications," *IEEE Trans. Power Electron.*, vol. 28, no. 4, pp. 1946–1960, Apr. 2013.
- [10] Y. Gu, L. Hang, Z. Lu, Z. Qian, and D. Xu, "Voltage doubler application in isolated resonant converters," in *Proc. 31st Annu. Conf. IEEE Ind. Electron. Soc. (IECON 2005)*, p. 5.